

ILC damping ring vacuum system design and instability modelling: possible applications to Super-B

Maxim Korostelev

University of Liverpool, and the Cockcroft Institute



Outline

- Lattice parameters and layout
- Mechanical design of vacuum system components
- Wake field calculations
- Instability modelling by parallel tracking code

LC - UK damping rings research goals

Lattice design (Maxim Korostelev, Andy Wolski, U.Liverpool and Cockcroft Institute)

Vacuum system technical design and magnet support structures (Oleg Malyshev, STFC/ASTeC
Norbert Collomb, John Lucas, Steve Postlethwaite, STFC/Technology)

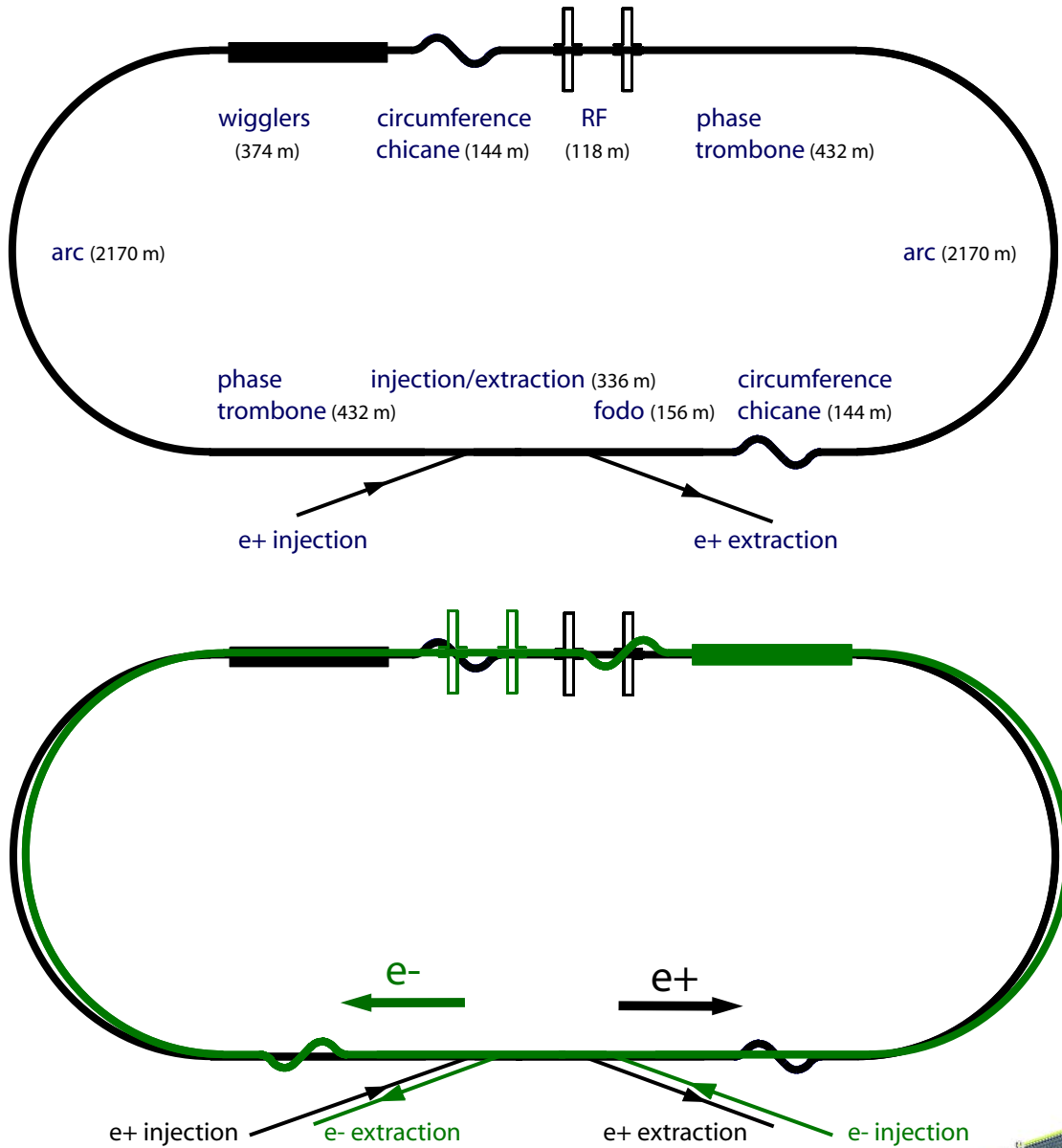
Impedance and single-bunch instability modelling (Maxim Korostelev, Alex Thorley, Andy Wolski
U.Liverpool and Cockcroft Institute)

Coupled bunch instabilities (Kai Hock, U.Liverpool and Cockcroft Institute)

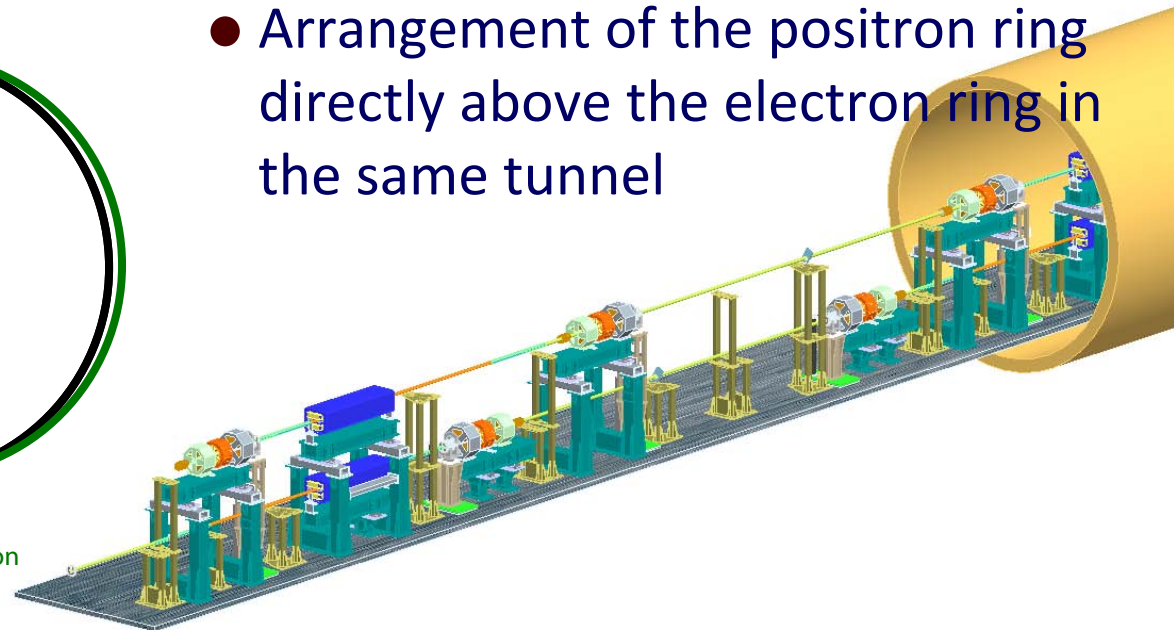
Low-emittance tuning (Kosmas Panagiotidis, Andy Wolski, U.Liverpool and Cockcroft Institute,
James Jones, STFC/ASTeC)

Coordination of LC-UK damping ring activity (Andy Wolski, U.Liverpool and Cockcroft Institute)

DCO4 layout of the ILC damping ring



- Energy of 5 GeV
- Circumference of 6.4 km, FODO arcs
- Long wiggler section provides fast radiation damping
- Identical lattice for both electron and positron damping rings
- Arrangement of the positron ring directly above the electron ring in the same tunnel



DCO4 lattice parameters and beam characteristics

| | |
|-------------------------|--------------------|
| Beam energy | 5 GeV |
| Circumference | 6476.4 m |
| RF frequency | 650 MHz |
| Harmonic number | 14042 |
| Average current | 400 mA |
| Bunch population | 2×10^{10} |
| Number of bunches | 2610 |
| Transverse damping time | 21.1 ms |
| Wiggler peak field | 1.6 T |
| Energy loss per turn | 10.23 MeV/turn |

| | | | |
|-----------------------------|-----------------------|-----------------------|-----------------------|
| Phase advance per arc cell | 72° | 90° | 100° |
| Momentum compaction | 2.9×10^{-4} | 1.6×10^{-4} | 1.3×10^{-4} |
| Normalized horiz. emittance | 6.4 μm | 4.4 μm | 3.9 μm |
| RMS bunch length | 6.0 mm | 6.0 mm | 6.0 mm |
| RMS energy spread | 1.27×10^{-3} | 1.27×10^{-3} | 1.27×10^{-3} |
| RF voltage | 32.6 MV | 20.4 MV | 17.1 MV |
| RF acceptance | 2.38 % | 1.96 % | 1.72 % |
| Synchrotron tune | 0.063 | 0.036 | 0.028 |
| Horizontal betatron tune | 61.12 | 71.12 | 76.12 |
| Vertical betatron tune | 60.41 | 71.41 | 75.41 |
| Natural horiz. chromaticity | -71.0 | -89.2 | -99.8 |
| Natural vert. chromaticity | -72.6 | -91.0 | -100.7 |

692 - quads, BPMs; 392 - sextupoles; 20 RF cavities

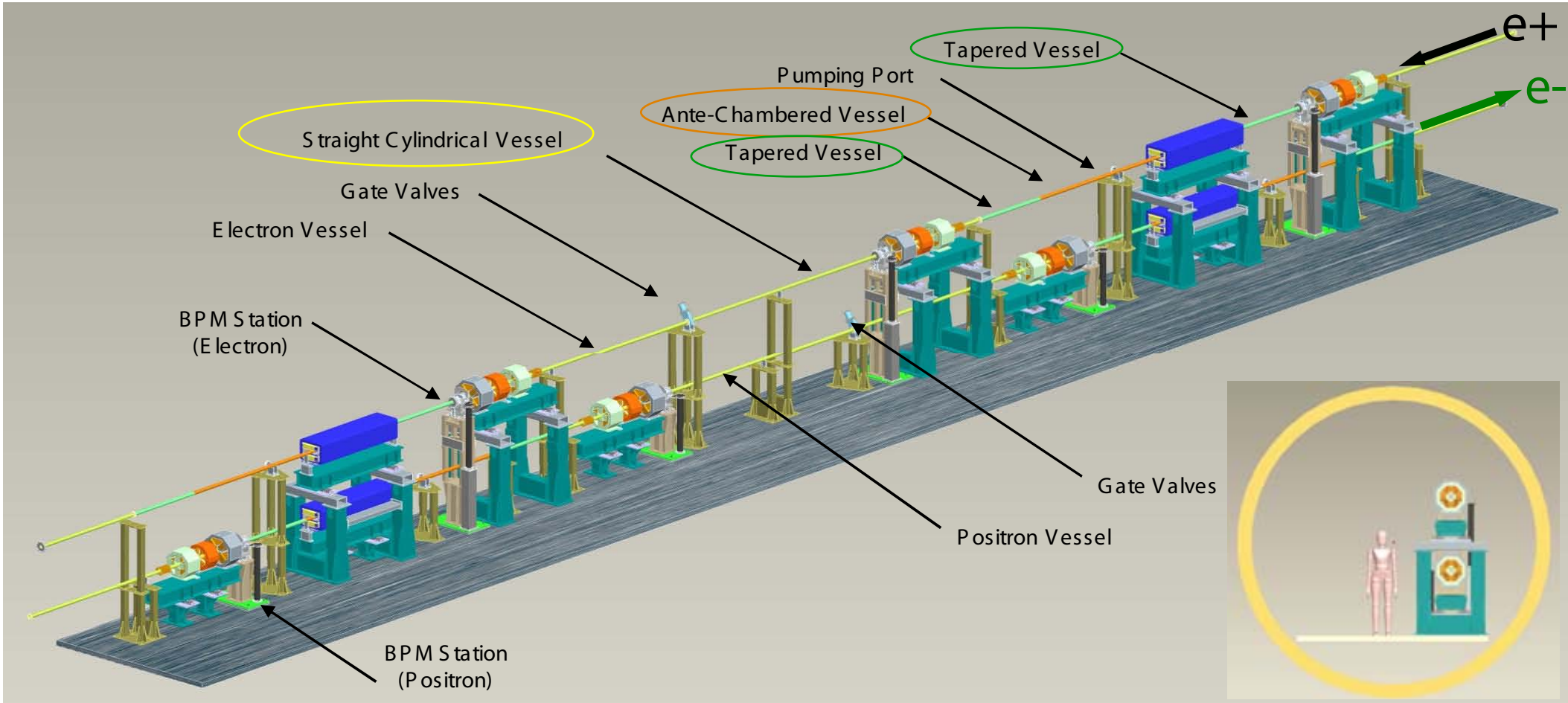
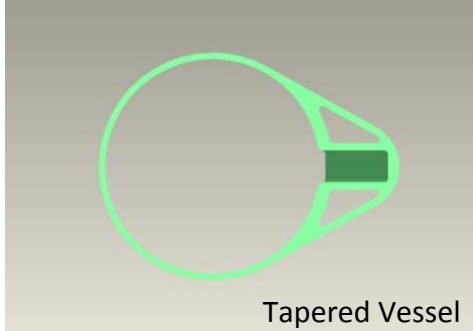
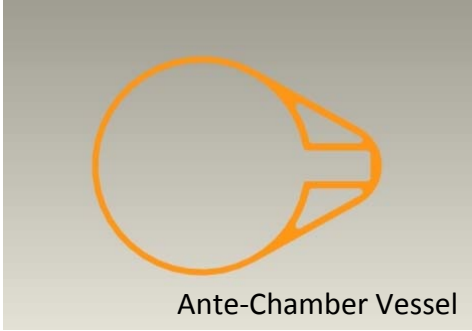
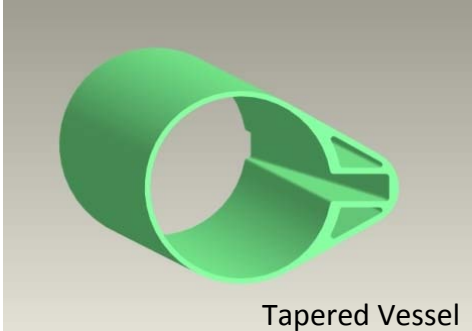
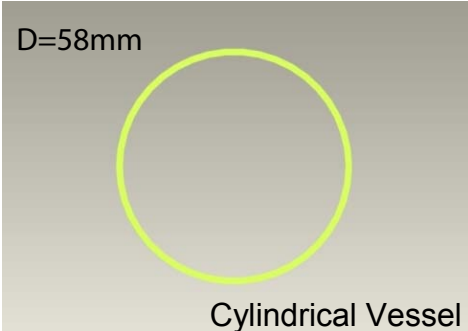
Choice of momentum compaction factor is a compromise between:

- beam emittance versus acceptance,
- required RF voltage versus instability thresholds

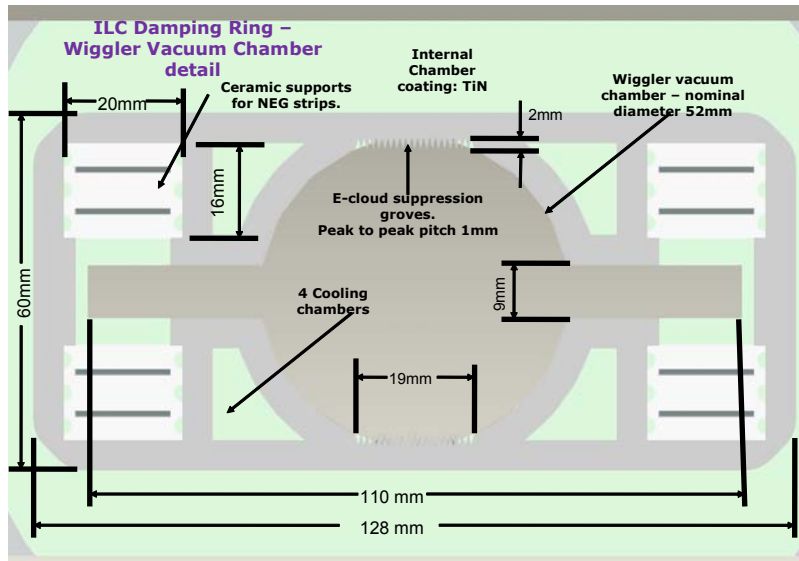
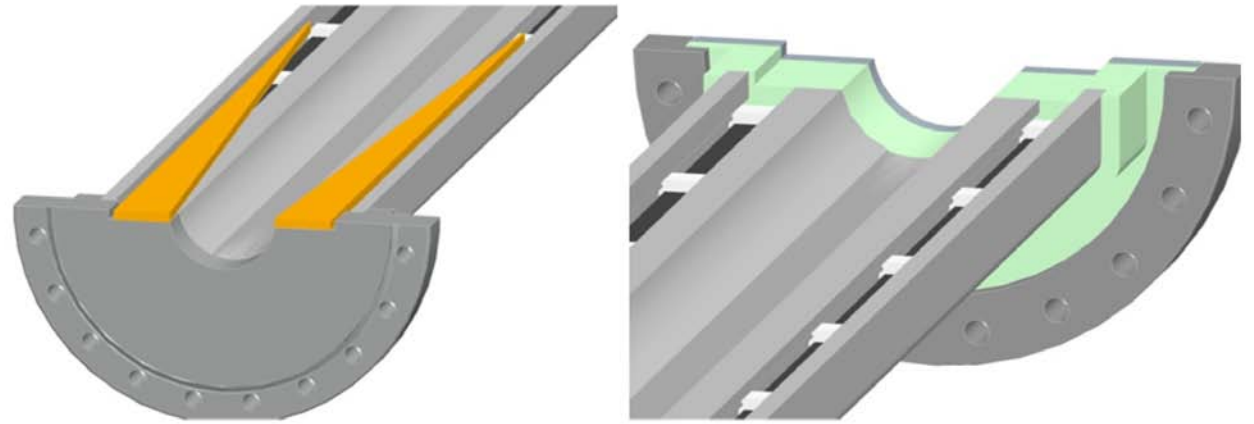
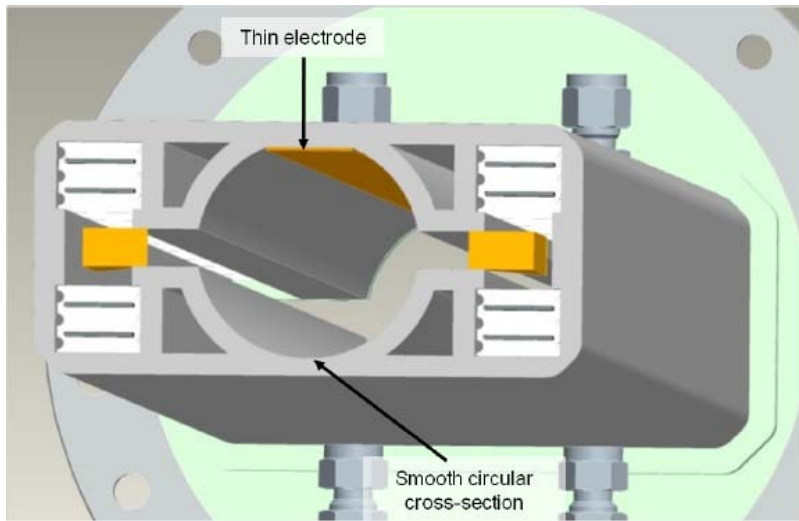
Damping ring vacuum system components

- Design work for a vacuum system components is generally focused on:
 - Vacuum chamber in the arcs
 - Vacuum chamber in the wiggler section
 - Insertions for beam position monitors (BPM)
 - Synchrotron radiation power absorbers
- to meet their key technical performance specifications
- to keep as low as possible the contribution to the overall machine impedance and impact on the beam dynamics

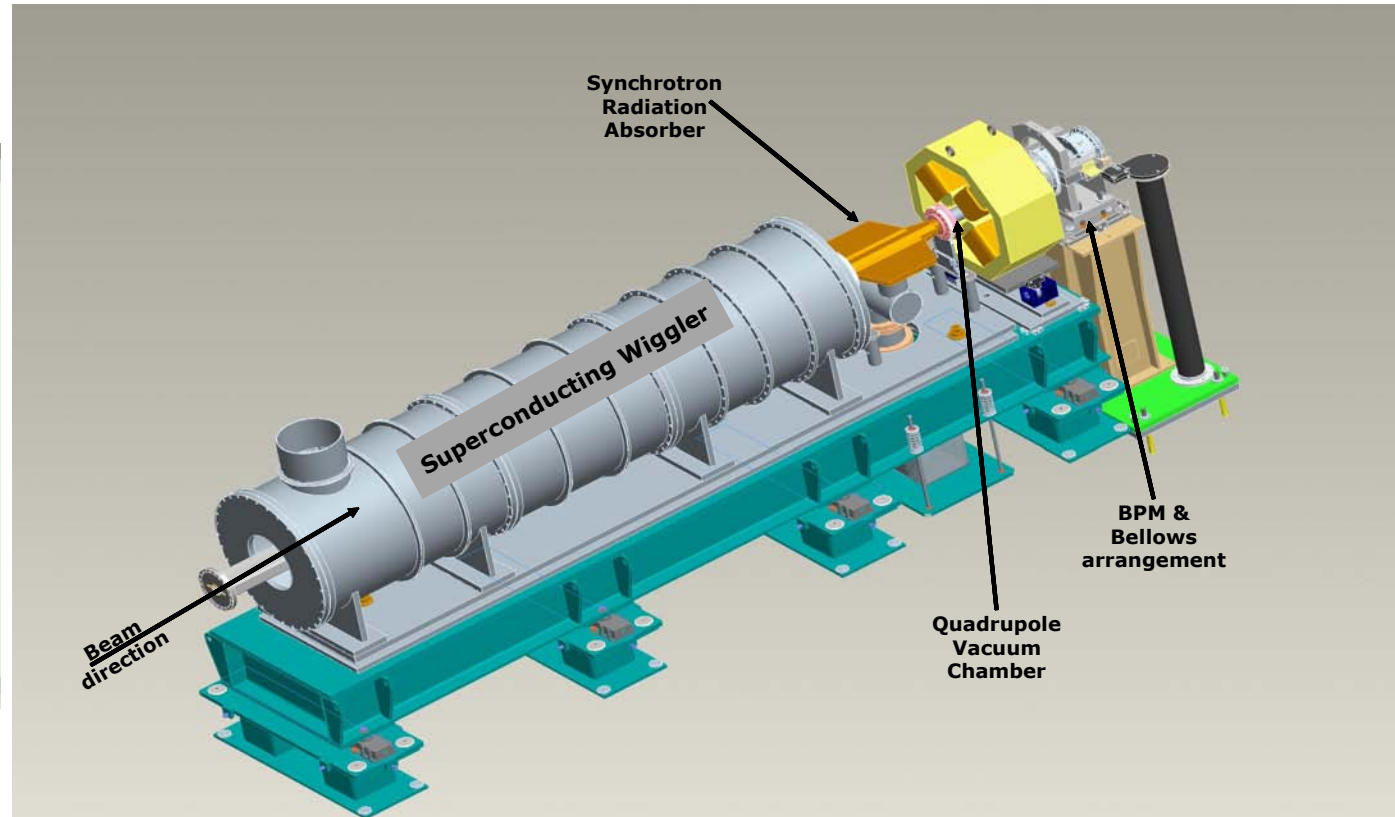
Vacuum chamber in the arcs



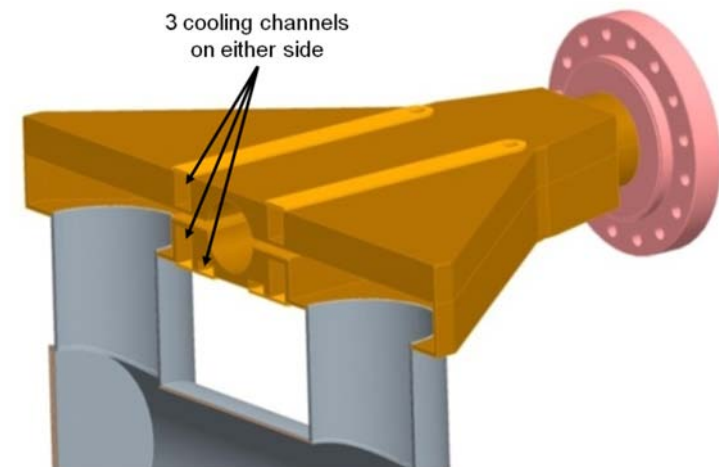
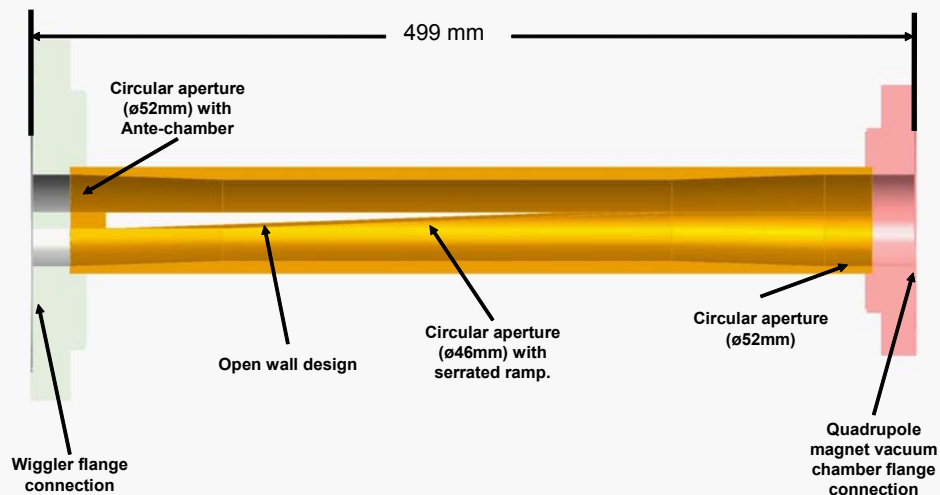
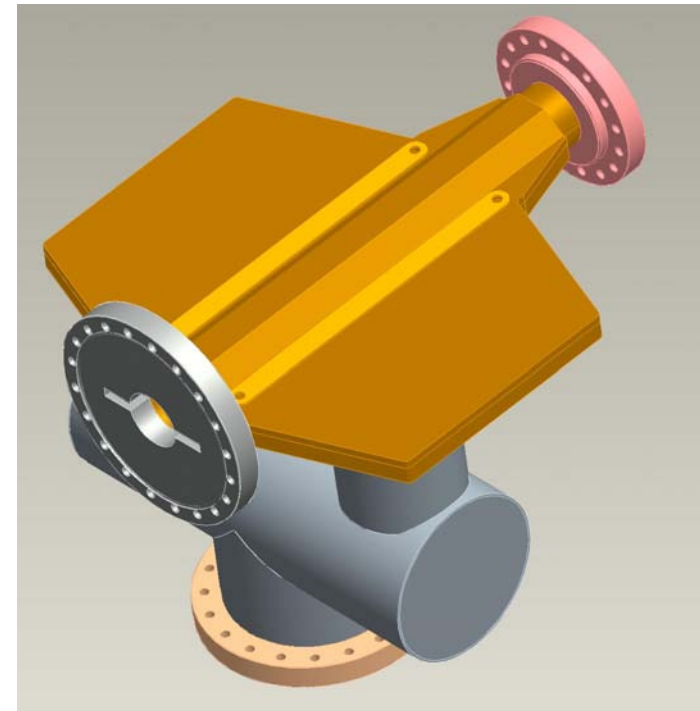
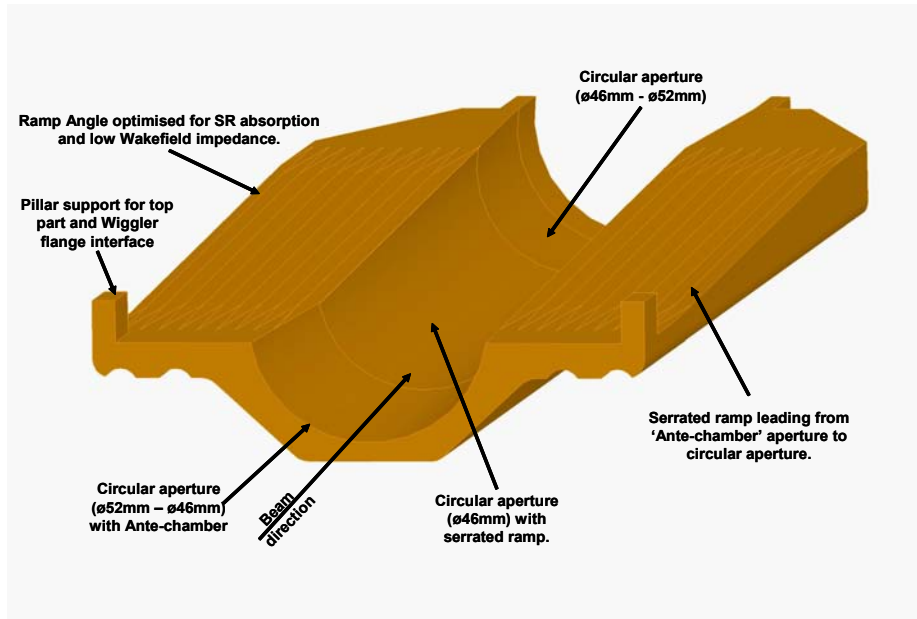
Vacuum chamber in the wiggler section



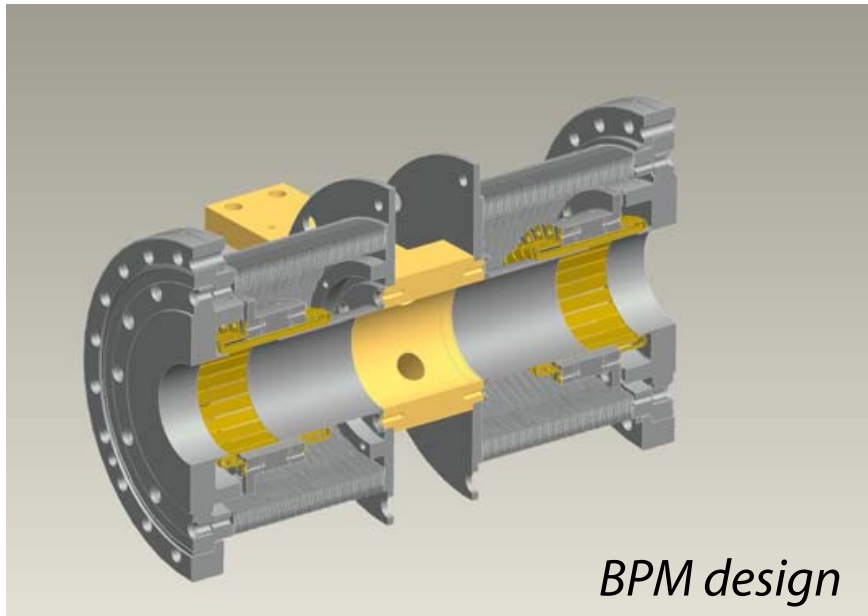
Wiggler vacuum chamber is based on a design by Cornell



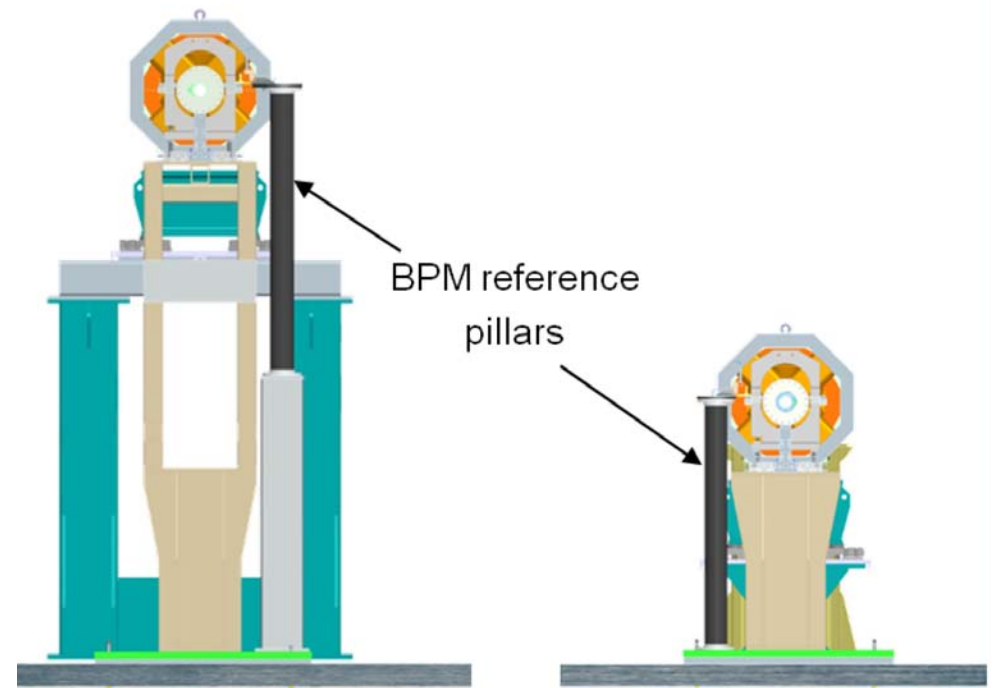
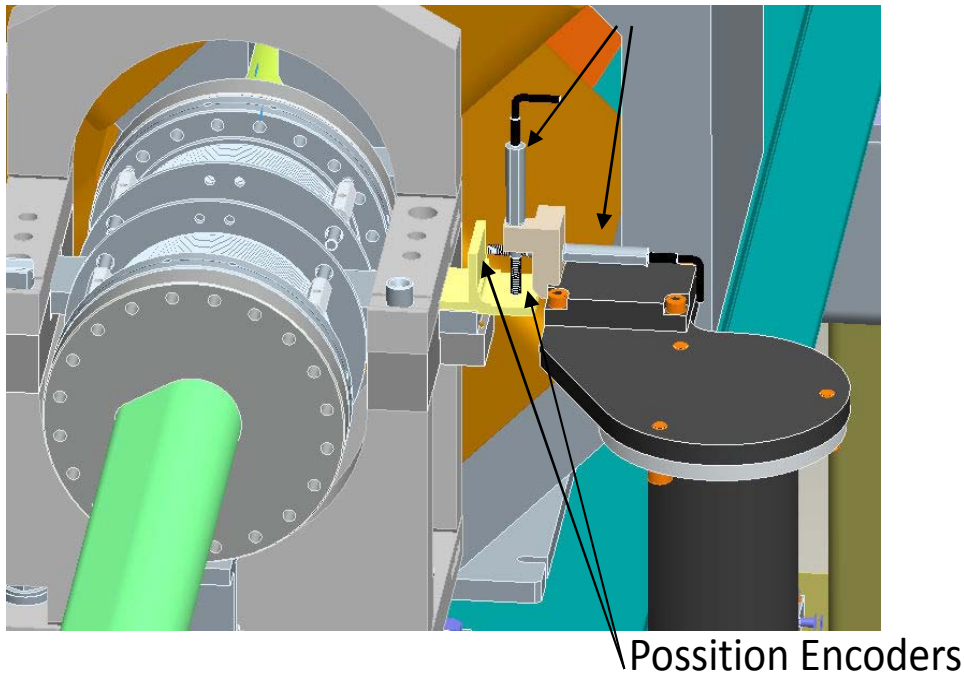
Synchrotron radiation power absorber



Insertion for BPM

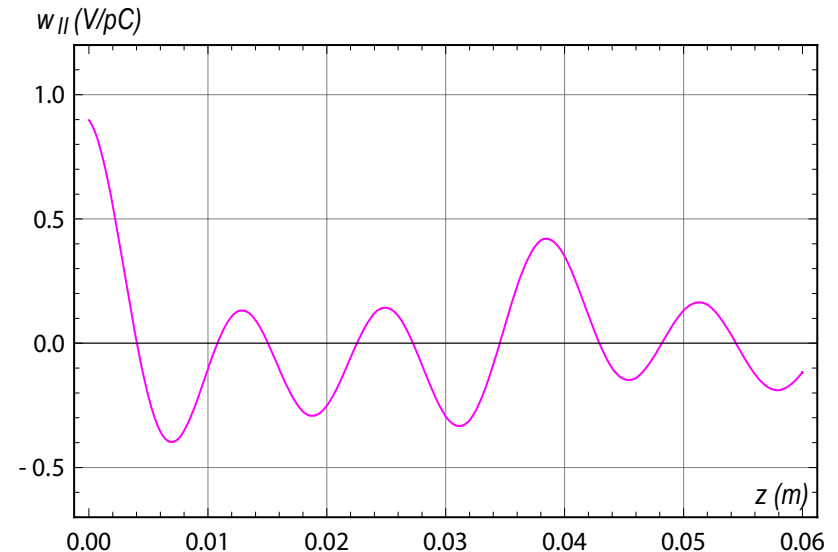
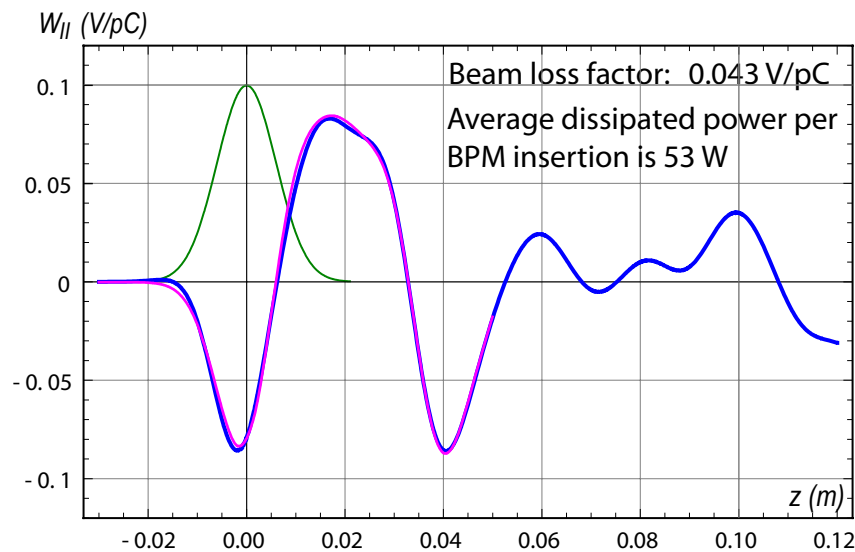
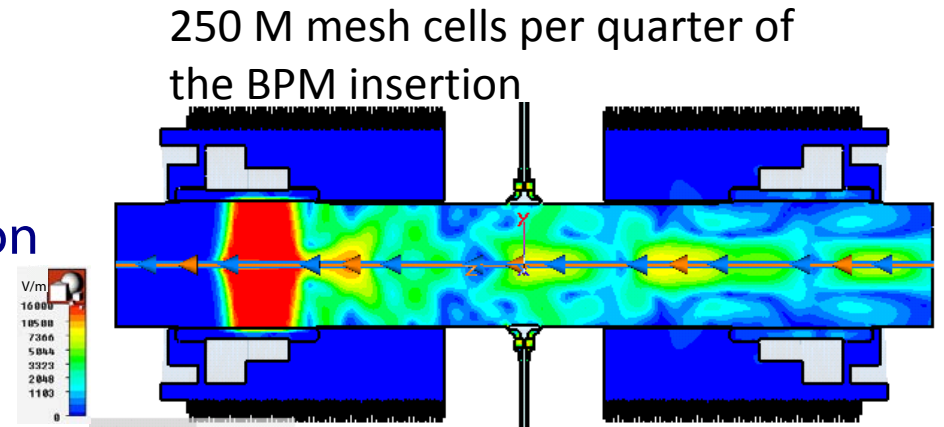


- Bellows design with multi-strip shield, based on a design from INFN-LNF has been implemented.
- BPM support system is based on the system used at the Diamond Light Source



Wake field 3D simulations for BPM insertion

- CST Particle Studio 3D time-domain simulations
- The simulations are based on the finite integration method.
- Hexagonal mesh is used to represent 3D model.

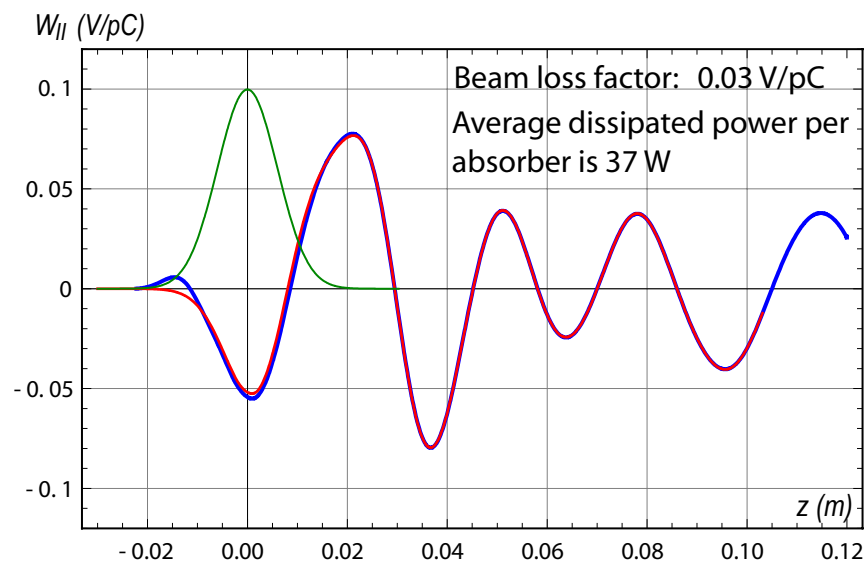


- Gaussian relativistic electron bunch with rms length of 6 mm.

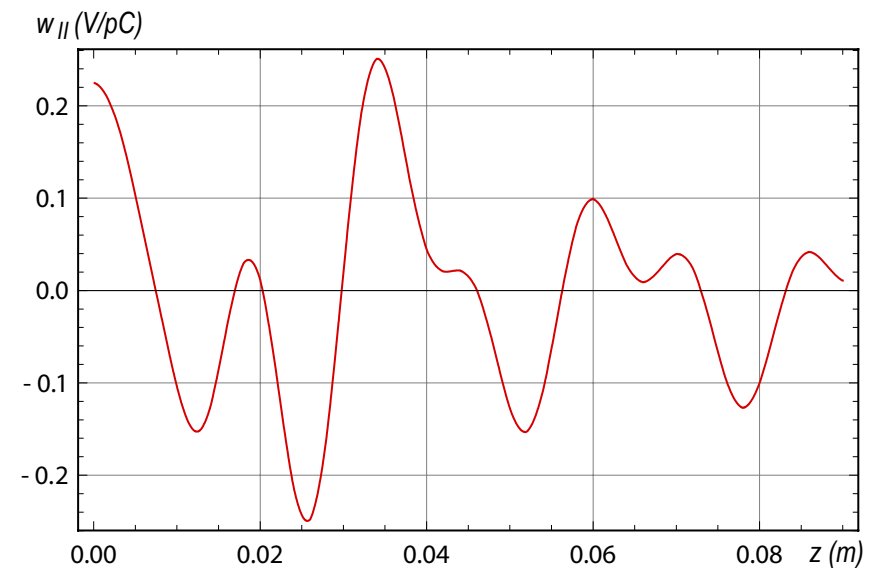
$$-cZ_{||}(\omega) = \frac{\int_{-\infty}^{\infty} W_{||}(z)e^{-i\frac{\omega z}{c}} dz}{\int_{-\infty}^{\infty} \lambda(z)e^{-i\frac{\omega z}{c}} dz} ; \quad w_{||}(z) = \frac{1}{2\pi c} \int_{-\infty}^{\infty} Z_{||}(\omega)e^{i\frac{\omega z}{c}} d\omega$$

Wake field 3D simulations for absorber

- CST Particle Studio 3D time-domain simulations



The longitudinal wake potential



The longitudinal wake function

- Gaussian relativistic electron bunch
with rms length of 6 mm.

Instability modelling by parallel tracking code

The bunch charge distribution is represented by a number of point-like macroparticles with equal charge.

Change in energy deviation of each macroparticle resulting from wake field

$$\Delta\delta_{pw}(z) = -\frac{QN_m r_e}{\gamma} \int_z^\infty \lambda(z') w_{||}(z - z') dz'$$

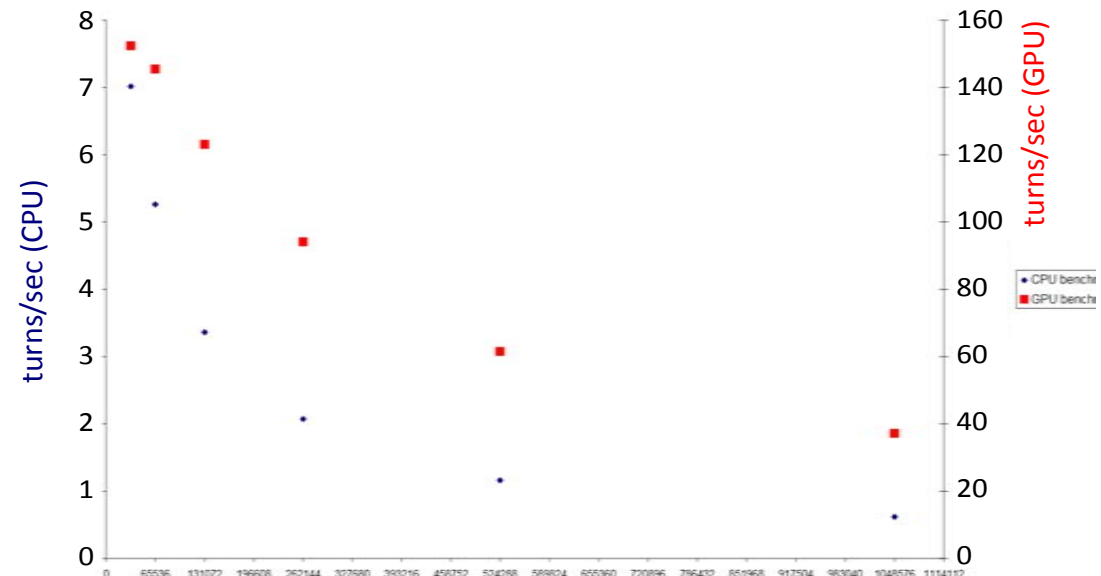
Macroparticle tracking running in parallel on a multi-core GPU

$$\delta_p^{n+1} = \delta_p^n + \frac{eV_{rf}}{E_0} \sin\left(\frac{\omega_{rf} z^n}{c}\right) - \frac{U_0}{E_0} (1 + \delta_p^n)^2 + \sigma_{pq}(u_c, \delta_p^n) + \Delta\delta_{pw}(z^n)$$

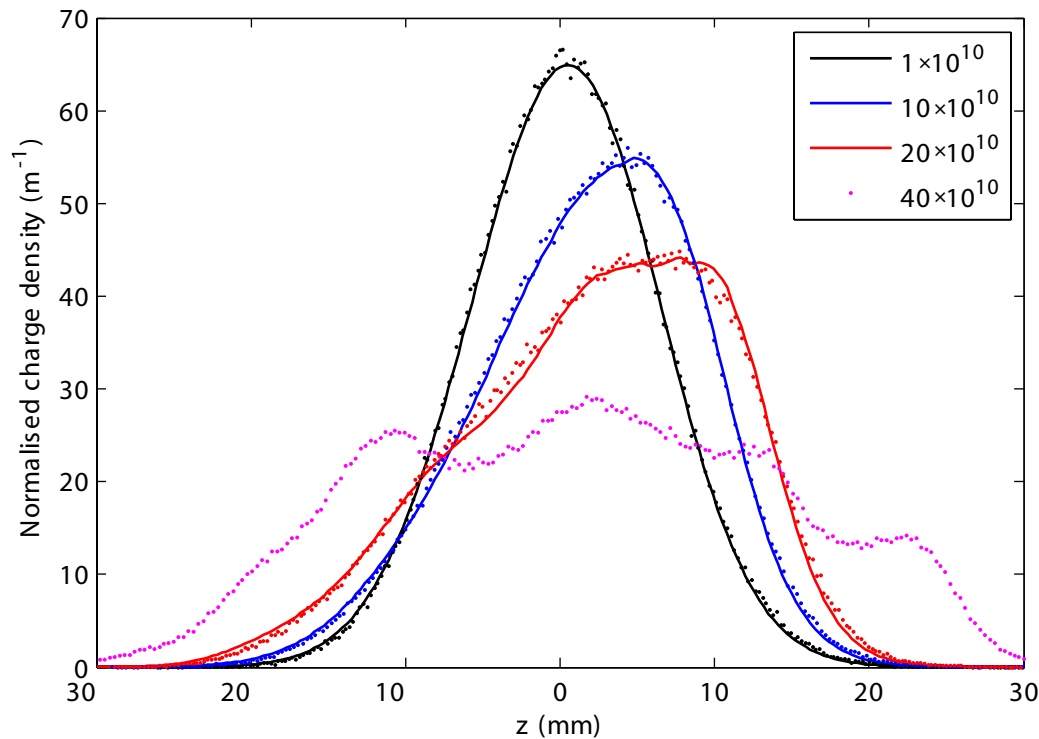
$$z^{n+1} = z^n - \alpha_p C \delta_p^{n+1}$$

Performance increase approximately 60x over the sequential processing of an equivalent code running on a CPU

Comparison of CPU vs GPU turn rate as a function of number of macroparticles

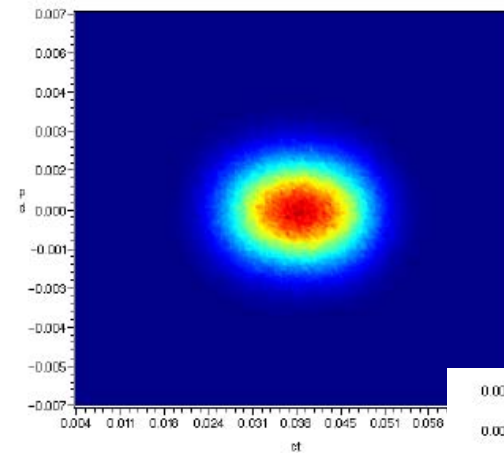


Results of tracking simulation vs solution of the Haissinski equation

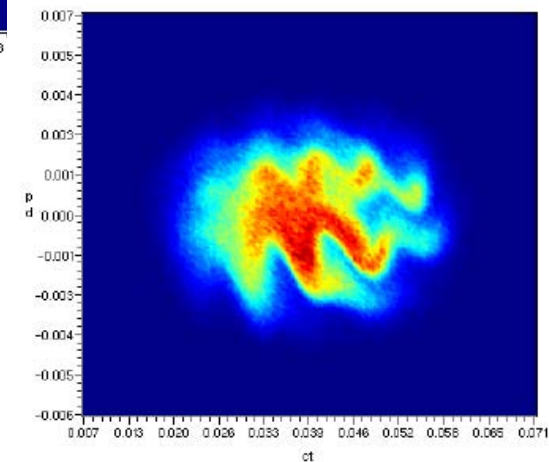


Below the instability threshold, the results of the tracking simulation for the longitudinal charge distribution are in a very good agreement with the solution of the Haissinski equation.

steady-state



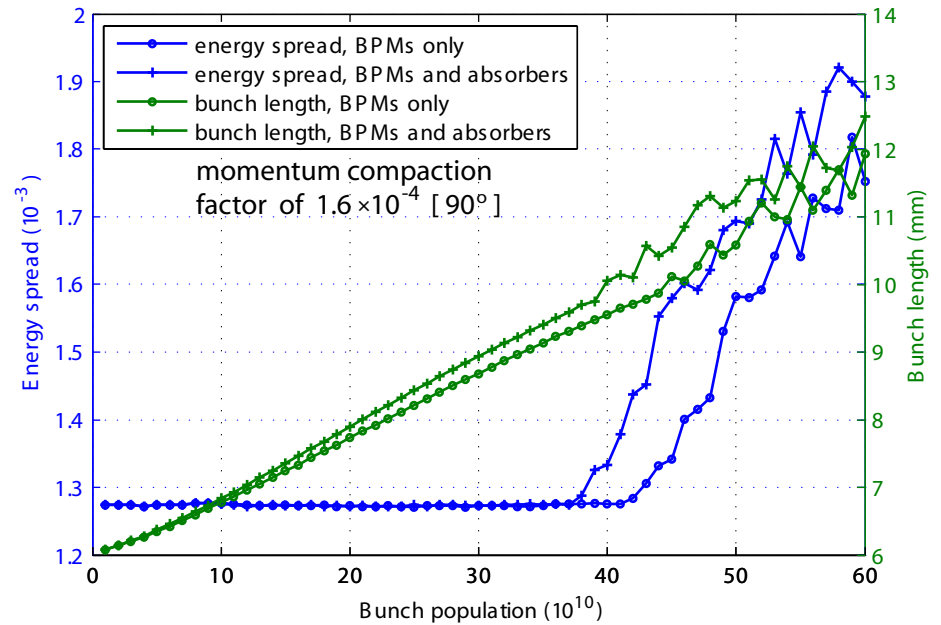
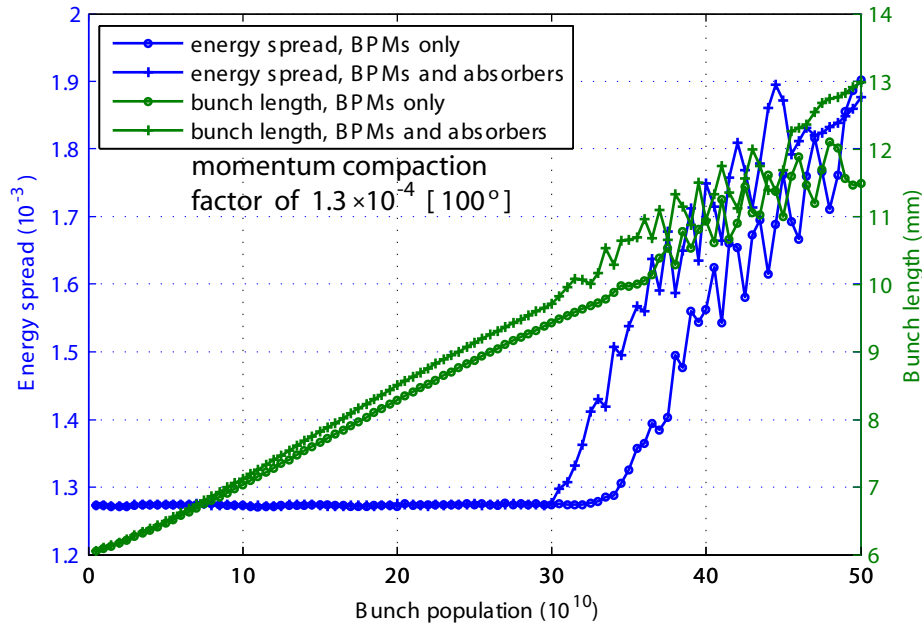
instability build-up



$$\lambda(z) = K \exp \left\{ -\frac{z^2}{2\sigma_z^2} - \frac{4\pi\epsilon_0 r_e N_b}{\alpha_p \gamma C \sigma_\delta^2} \int_0^z W_{\parallel}(z') dz' \right\}$$

$$\int_{-\infty}^{\infty} \lambda(z) dz = 1; W_{\parallel}(z') = \int_{z'}^{\infty} \lambda(z'') w_{\parallel}(z' - z'') dz''$$

Single-bunch instability threshold



The instability threshold is $\sim 33 \times 10^{10}$ in the presence of the BPM wake field only.

The instability threshold is $\sim 30 \times 10^{10}$ in the presence of the BPM wake field AND wake field from the absorbers.

In the case that only the BPM insertions are included, the effective value of $|Z/n|$ is $10 \text{ m}\Omega$; this rises to $12 \text{ m}\Omega$ if the absorbers are included.

$$\left| \frac{Z_{\parallel}}{n} \right| < \sqrt{\frac{\pi}{2}} Z_0 \frac{\gamma \alpha_p \sigma_{\delta}^2 \sigma_z}{r_e N_0}$$

To remain below the instability threshold for the nominal maximum bunch population of 2×10^{10} particles, the effective broadband impedance should not exceed $235 \text{ m}\Omega$, $130 \text{ m}\Omega$ and $105 \text{ m}\Omega$ for the lattices with momentum compaction factor 2.9×10^{-4} , 1.6×10^{-4} and 1.3×10^{-4} , respectively.

Conclusion

- The lattice and technical design validate for significant performance criteria, including low emittance tuning, short range wake fields and single bunch instability thresholds.
- A parallel tracking code has been developed for studies of bunch lengthening and single-bunch instability: a performance increase 60x over the sequential processing on a CPU.
- The tracking simulations are in very good agreement with analytical predictions from the Haissinski equation.
- The lowest instability threshold is more than an order of magnitude larger than the bunch population specified for the damping ring.
- Design of the synchrotron radiation power absorber, BPM insertion, vacuum vessels in a dipoles and wigglers provide sufficient margin in impedance for the rest of the vacuum system such as RF cavities and kickers.